The Active-Site Histidine-10 of Enterococcal NADH Peroxidase Is Not Essential for Catalytic Activity†

Edward J. Crane, III,‡ Derek Parsonage,‡ and Al Claiborne*

Department of Biochemistry, Wake Forest University Medical Center, Winston-Salem, North Carolina 27157

Received October 2, 1995; Revised Manuscript Received December 21, 1995⊗

ABSTRACT: In order to test the proposal [Stehle, T., Claiborne, A., & Schulz, G. E. (1993) *Eur. J. Biochem. 211*, 221−226] that the active-site His10 of NADH peroxidase functions as an essential acid−base catalyst, we have analyzed mutants in which this residue has been replaced by Gln or Ala. The k_{cat} values for both H10Q and H10A peroxidases, and the pH profile for k_{cat} with H10Q, are very similar to those observed with wild-type peroxidase. Both mutants, however, exhibit $K_m(H_2O_2)$ values much higher (50−70-fold) than that for wild-type enzyme, and stopped-flow analysis of the H_2O_2 reactivity of two-electron reduced H10Q demonstrates that this difference is due to a 150-fold decrease in the second-order rate constant for this reaction with the mutant. Stopped-flow analyses also confirm that reduction of the enzyme by NADH is essentially unaffected by His10 replacement and remains largely rate-limiting in turnover; the formation of an E·NADH intermediate in the conversion of E→EH_2 is confirmed by diode-array spectral analyses with H10A. Both H10Q and H10A mutants, in their oxidized E(FAD, Cys42-sulfenic acid) forms, exhibit enhanced long-wavelength absorbance bands (λ_{max} = 650 nm and 550 nm, respectively), which most likely reflect perturbations in a charge-transfer interaction between the Cys42-sulfenic acid and FAD. Combined with the 50-fold increase in the second-order rate constant for H_2O_2 inactivation (via Cys42-sulfenic acid oxidation) of the H10Q mutant, these observations support the proposal that His10 functions in part to stabilize the unusual Cys42-sulfenic acid redox center within the active-site environment.

Although structurally related to flavoprotein disulfide reductases such as glutathione reductase (GR;[1] Williams, 1992), the NADH peroxidase from *Enterococcus faecalis* 10C1 is unique in that it utilizes the Cys42 thiol/sulfenic acid (−SH/−SOH) redox couple in the heterolytic cleavage of the peroxide bond (Claiborne et al., 1993, 1994). Recent studies from this laboratory not only have documented the essential role of Cys42 in the catalytic redox cycle (Parsonage & Claiborne, 1995) but also have investigated the properties of an L40C mutant which contains an active-site Cys40−Cys42 disulfide (Miller et al., 1995). The kinetic mechanism of the wild-type peroxidase has been shown (Crane et al., 1995) to involve (1) NADH reduction of E(FAD, Cys42-SOH)→EH_2(FAD, Cys42-SH) in an initial priming step; (2) rapid binding of NADH to EH_2; (3) reduction of H_2O_2 by the Cys42-thiolate, yielding E·NADH; and (4) rate-limiting hydride transfer from bound NADH, regenerating EH_2. No discrete $FADH_2$ intermediate has been observed, however, and the precise details of Cys42-SOH reduction have not been elucidated. The pH profile for k_{cat} reveals a relatively acidic optimum of 5.0−5.5 with an apparent limiting pK_a of 6.9, consistent with the requirement for a proton in the rate-limiting hydride transfer step.

The active-site base in *Escherichia coli* GR is His439 (Greer & Perham, 1986; Mittl & Schulz, 1994), which is located near the C-terminus of the complementary subunit and interacts with the Cys42−Cys47 redox-active disulfide of the reference subunit. Recent studies of the H439A mutant (Rietveld et al., 1994) have shown that this protein has only 0.3% residual activity; specifically, the limiting rate of GSSG reduction by the corresponding EH_2 species is decreased by approximately 4800-fold. Rietveld et al. (1994) have suggested that His439 serves, in the oxidative half-reaction, to protonate the nascent thiolate of the first GSH product (pK_a = 9.7; Dawson et al., 1986), thus preventing the reverse reaction. In contrast to the GR active-site histidine, His10 of the NADH peroxidase is located near the N-terminus of the α1 helix within the FAD-binding $\beta\alpha\beta$-fold and interacts with Cys42 (observed in the crystal structure as the non-native Cys42-sulfonic acid; Cys42-SO_3H) of the same subunit within the tetrameric enzyme (Stehle et al., 1991, 1993). Among the six partial and complete NADH peroxidase and NADH oxidase sequences available (Ross & Claiborne, 1991, 1992; Miller et al., 1990; Matsumoto et al., 1995; Fraser et al., 1995; GenBank Accession Number U19610), His10 is absolutely conserved. Stehle et al. (1993), on the basis of the active-site structure of the NADH peroxidase E(Cys42-SO_3H) complex with NADH, proposed that His10 protonates the nascent hydroxide ion (pK_a = 15.7; March, 1985) formed on reduction of H_2O_2 by the EH_2 Cys42-thiolate. This proposal has been brought into question more recently, however, by the

† This work was supported by National Institutes of Health Grant GM-35394. E.J.C. is the recipient of National Research Service Award GM-16274.

* To whom correspondence should be addressed at the Department of Biochemistry, Wake Forest University Medical Center, Medical Center Blvd., Winston-Salem, NC 27157. Telephone: (910) 716-3914. Fax: (910) 716-7671. URL: http://invader.bgsm.wfu.edu:80/.

‡ These authors contributed equally to this work.

⊗ Abstract published in *Advance ACS Abstracts,* February 1, 1996.

[1] The abbreviations: GR, glutathione reductase; E, oxidized enzyme; EH_2, two-electron reduced enzyme; EH_4, four-electron reduced enzyme; Cys42-SOH, Cys42-sulfenic acid; Cys42-SO_3H, Cys42-sulfonic acid derivative observed in peroxide-inactivated peroxidase; IPTG, isopropyl β-D-thiogalactopyranoside; E'^0, midpoint redox potential at pH 7.0; E_1, midpoint potential for the redox couple EH_2/EH_4; E_2, midpoint potential for the redox couple E/EH_2.

observation of a hydrogen bond between the Arg303 guanidinium moiety and the His10 imidazole in the NADH peroxidase C42S mutant structure; a similar interaction is also present in the wild-type enzyme (Mande et al., 1995). Mande et al. (1995) have concluded that His10 very likely remains unprotonated throughout the catalytic cycle.

Sulfenic acids in solution are generally unstable; intramolecular hydrogen bonding between R-SOH and a suitable hydrogen bond acceptor represents one mechanism for stabilization (Claiborne et al., 1993; Tripolt et al., 1993). The crystal structure of the NADH peroxidase Cys42-SO_3H form demonstrates that one of the oxygen atoms (OX1) of Cys42-SO_3H is hydrogen-bonded both to the His10 imidazole and to Cys42-N; on this basis, Stehle et al. (1993) concluded that OX1 corresponds to the sulfenic acid oxygen of the native peroxidase (Cys42-SOH form), and we have extended this to suggest (Claiborne et al., 1993) that His10 functions in part to stabilize the unusual Cys42-SOH redox center. In order to investigate the role of His10 in more detail, we have analyzed the kinetic, spectral, and redox properties of H10Q and H10A mutants of the peroxidase, and these results form the basis of this report.

EXPERIMENTAL PROCEDURES

Materials and General Methods. NAD^+, $NADP^+$, NADH, and NADPH were purchased from Boehringer Mannheim, and hydrogen peroxide (30%) was from Mallinckrodt. (4*S*)-[4-^{1}H]- and (4*S*)-[4-^{2}H]NADH were prepared as described recently (Crane et al., 1995). All other chemicals, as purchased from the sources given previously (Parsonage & Claiborne, 1995), were of the best grades available. General protocols for anaerobic spectral titrations and for stopped-flow kinetic analyses have been described (Parsonage & Claiborne, 1995; Crane et al., 1995), and the procedures used for DNA isolation and manipulation, mutagenesis, and expression have also been reported previously (Parsonage & Claiborne, 1995; Miller et al., 1995).

Mutagenesis and Expression. The H10Q mutation was generated in the plasmid pNPX14, as described recently for the NADH peroxidase S38C and S41C mutants (Miller et al., 1995). The 160 bp *Sal*I−*Sph*I fragment from the mutant plasmid was ligated into pNPX9 to give the pH10Q expression plasmid. The H10A mutation was generated in the plasmid pNPR4 (Parsonage et al., 1993), following the protocol described for the C42S and C42A mutants (Parsonage & Claiborne, 1995). The 159 bp *Ssp*I−*Sph*I fragment of the mutant plasmid was then transferred to pNPX9 via an intermediary pBluescript plasmid, as described for the generation of pNPX9 (Parsonage et al., 1993), to give the pH10A expression plasmid. Both final plasmids, pH10Q and pH10A, were checked by sequence and restriction analyses. The corresponding H10Q and H10A mutant proteins were expressed in *Escherichia coli* JM109DE3 on induction with IPTG and were purified using the procedure developed for wild-type recombinant NADH peroxidase (Parsonage et al., 1993).

Diode-Array Analysis. Rapid-reaction studies using a Hi-Tech SF-61 stopped-flow apparatus equipped with a diode-array detector were carried out with the H10A mutant in the laboratory of Dr. David P. Ballou at the University of Michigan, as described previously (Crane et al., 1995; Gassner & Ballou, 1995).

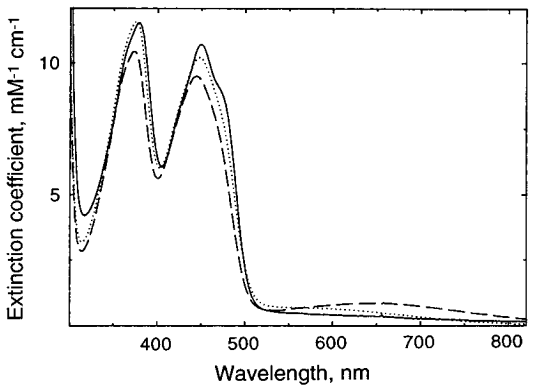

FIGURE 1: Comparison of the visible absorption spectrum of oxidized wild-type NADH peroxidase (—) with those of H10Q (− −) and H10A (•••) mutant enzymes. Spectra shown represent the proteins in 50 mM potassium phosphate, pH 7.0, plus 0.6 mM EDTA, at 23 °C.

RESULTS

Purification and Spectral Properties. The H10Q and H10A peroxidase mutants were expressed and purified using procedures described previously for C42S and other mutant enzymes (Parsonage & Claiborne, 1995; Miller et al., 1995), although lower yields of ~25 mg from 3 L of recombinant *Escherichia coli* were routinely observed for both His10 mutants. Both proteins contain tightly-bound FAD, and the flavin fluorescence of the H10Q mutant is strongly quenched, as seen with wild-type peroxidase (Poole & Claiborne, 1986). H10Q also purified on occasion as a mixture of oxidized E(FAD, Cys42-SOH) and EH_2(FAD, Cys42-SH) forms; titration with H_2O_2 regenerated the fully oxidized enzyme directly. Figure 1 gives the visible absorption spectra of wild-type recombinant NADH peroxidase (λ_{max} = 380, 450 nm; ϵ_{450} = 10 900 M^{-1} cm^{-1}), the H10Q mutant (λ_{max} = 374, 444 nm; ϵ_{444} = 9 800 M^{-1} cm^{-1}), and the H10A mutant (λ_{max} = 376, 448 nm; ϵ_{448} = 10 300 M^{-1} cm^{-1}). The absorbance ratios at 280 and 450 nm for the purified enzymes are 7.8, 8.7, and 8.6, respectively. The very low-extinction, long-wavelength absorbance band extending to 700 nm in the wild-type peroxidase has been attributed to a weak charge-transfer interaction between the electron-rich sulfenic acid oxygen and the oxidized flavin (Poole & Claiborne, 1989a). As shown in Figure 1, both H10Q and H10A peroxidase mutants have enhanced long-wavelength absorbance bands (λ_{max} = 650 and 550 nm, respectively) in their oxidized E(FAD, Cys42-SOH) forms. These spectral features are not due to the presence of either residual reduced enzyme or complexes with pyridine nucleotides, and this was further demonstrated by the fully reversible reduction and reoxidation observed with NADH and H_2O_2. Relative to the oxidized wild-type enzyme, both His10 mutant spectra lack the resolved shoulder at 472 nm, and in general their properties resemble those of the wild-type EH_2 form (Poole & Claiborne, 1986) over the range 300−500 nm, perhaps reflecting the enhanced Cys42-SOH→FAD interaction.

Reductive Titrations. Anaerobic dithionite titration of the oxidized H10Q mutant proceeded in two phases corresponding to the formation of the EH_2(FAD, Cys42-SH) and EH_4($FADH_2$, Cys42-SH) species (Figure 2). The first phase required 0.74 equiv of dithionite/FAD and led to a characteristic EH_2 spectrum with a new long-wavelength absorbance maximum at 535 nm; there is an isosbestic point at

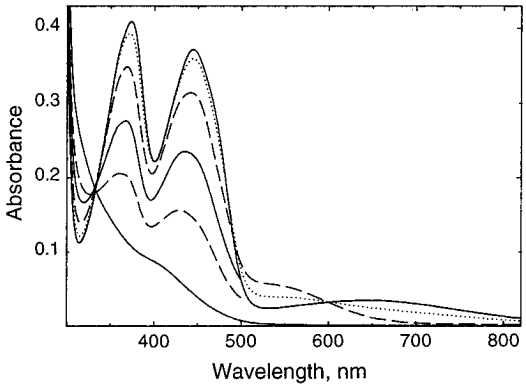

FIGURE 2: Anaerobic dithionite titration of the H10Q peroxidase. The cuvette contained 23.3 nmol of the H10Q mutant (FAD) in 0.6 mL of the standard pH 7.0 phosphate buffer containing EDTA. Spectra shown, in order of decreasing absorbance at 444 nm, correspond to the addition of 0 (—), 0.3 (···), 0.74 (− −), 1.03 (—), 1.33 (− −), and 2.07 (—) equiv of dithionite/FAD. Partial spectra (300−500 nm) are shown from the second phase of the titration, in order to avoid overlap with the long-wavelength bands of E and EH_2, which are given.

600 nm beyond which reduction of the Cys42-SOH center can be followed directly. There is only slight reduction of the oxidized flavin absorbance at this stage. From the structure of the wild-type peroxidase E(Cys42-SO_3H)·NADH complex, Stehle et al. (1993) observed that His10-NE2 and Cys42-SG are separated by 3.7 Å and suggested that a protonated His10 might form an ion pair with the Cys42-thiolate. In wild-type EH_2, the pK_a for Cys42-SH is ≤4.5, as is required in order to yield the 540 nm charge-transfer band attributed to the Cys42-S^-→FAD interaction (Poole & Claiborne, 1986). Over the pH range 5.4−7.1, however, there is no spectral evidence for an elevated Cys42 pK_a in the EH_2 form of the H10Q mutant; the Cys42-SH pK_a must still be ≤4.5. A similar titration of oxidized H10Q revealed no change in the 650 nm band attributed to Cys42-SOH, either. If this spectral feature does require a Cys42-SO^-→FAD interaction, then the pK_a of Cys42-SOH in the H10Q mutant must be ≤4.5 as well.

Dithionite titration of the H10Q EH_2 form requires 0.97 equiv of reductant/FAD and leads to the fully reduced EH_4 state. In contrast to the wild-type enzyme, the reduced H10Q spectrum lacks the 360 nm absorbance maximum which has been attributed to stabilization of the N(1)-anionic form of the dihydroflavin (Poole & Claiborne, 1989b); this difference may contribute to the 25−30 min equilibrations required during this stage of the H10Q reductive titration. Dithionite titration of the H10A peroxidase followed essentially the same course as described for H10Q.

Figure 3 gives the results of anaerobic NADH titrations of both H10Q and H10A peroxidases. In the case of the H10Q mutant, the sample was first titrated with H_2O_2 to generate the fully oxidized enzyme. As described for the dithionite titration of H10Q, the first phase of the NADH titration leads directly to the EH_2 form. In contrast, however, further additions of NADH do not lead to the fully reduced enzyme, but yield instead a stable EH_2·NADH complex similar to that described for wild-type peroxidase (Parsonage et al., 1993). The H10Q EH_2·NADH complex is characterized by absorbance maxima at 350, 440, and 535 nm. Although there is very low-extinction, long-wavelength absorbance beyond 650 nm, absorbance in this region is significantly diminished relative to that of the wild-type

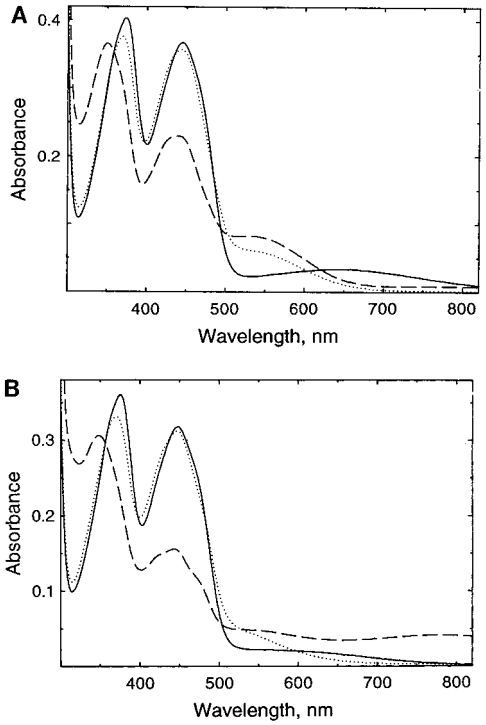

FIGURE 3: Anaerobic titrations of H10Q and H10A peroxidases with NADH. (A) The anaerobic cuvette contained 24.2 nmol of the H10Q mutant (FAD) in 0.63 mL of the standard pH 7.0 phosphate buffer containing EDTA. Spectra shown correspond to the addition of 0 (—), 0.59 (···), and 1.53 (− −) equiv of NADH/FAD. (B) The anaerobic cuvette contained 20.3 nmol of the H10A mutant (FAD) in 0.65 mL of the same buffer given in (A), and the spectra shown correspond to the addition of 0 (—), 0.92 (···), and 2.95 (− −) equiv of NADH/FAD. In both cases, an oxygen-scrubbing system consisting of protocatechuate dioxygenase and protocatechuic acid (Bull & Ballou, 1981) was added anaerobically prior to the titration.

EH_2·NADH form. NADH titration of the H10A peroxidase yields EH_2 and EH_2·NADH forms corresponding to the addition of 0.96 and 2.22 equiv of NADH/FAD, respectively. The H10A EH_2·NADH complex has absorbance maxima at 348, 445, 545, and 775 nm and more closely resembles the wild-type EH_2·NADH spectrum.

The extinction coefficients at 440−445 nm for the H10Q and H10A EH_2·NADH species are 65% and 49%, respectively, those of the oxidized enzymes, raising the possibility of significant spectral contributions by the corresponding EH_4·NAD^+ complexes. While we have shown (Crane et al., 1995) that anaerobic NAD^+ titration of the wild-type peroxidase EH_4 species leads to the stoichiometric (with added NAD^+) appearance of EH_2·NADH, a similar titration of the reduced C42S peroxidase mutant does give rise to the stable $FADH_2$·NAD^+ charge-transfer complex (Parsonage & Claiborne, 1995). Given the spectral differences between the EH_4 and EH_2·NADH forms of the H10Q peroxidase documented in Figures 2 and 3, we determined whether the H10Q EH_4·NAD^+ complex contributes significantly to the EH_2·NADH spectrum. When the dithionite-reduced H10Q peroxidase is titrated anaerobically with NAD^+ (Figure 4), there is stoichiometric (with added NAD^+) formation of an enzyme species with spectral properties virtually identical to those of the H10Q EH_2·NADH complex given in Figure 3. The absorbance maximum at 353 nm is consistent with the presence of bound NADH, and the λ_{max} values at 435 and 525 nm are characteristic of the Cys42-S^-→FAD charge-

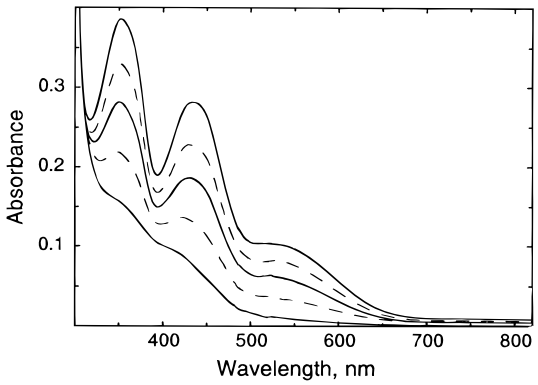

FIGURE 4: Anaerobic NAD^+ titration of H10Q peroxidase EH_4. The cuvette contained 24.2 nmol of enzyme in 0.7 mL of the pH 7.0 phosphate buffer, including 0.1 M potassium acetate. The EH_4 form was generated by titrating the oxidized H10Q mutant with 2.2 equiv of dithionite/FAD. The dithionite syringe was then exchanged for one containing an anaerobic NAD^+ solution. Spectra shown, in order of increasing absorbance at 440 nm, represent EH_4 (—) and EH_4 plus 0.22 (− −), 0.59 (—), 1.03 (− −), and 3.67 (—) equiv of NAD^+/FAD.

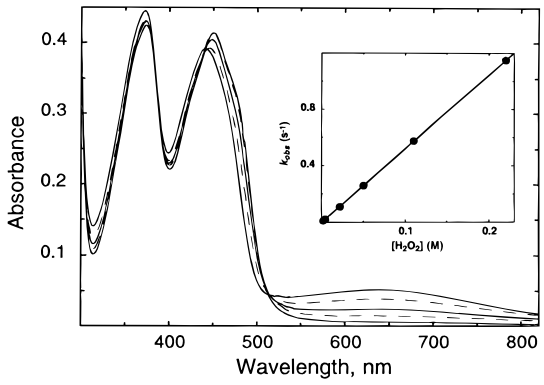

FIGURE 5: Spectral course of peroxide inactivation of H10Q peroxidase. The cuvette contained 27.8 nmol of enzyme (—) in 0.7 mL of the pH 7.0 phosphate/acetate buffer at 23 °C. The reaction was initiated by adding H_2O_2 to a final concentration of 2.3 mM, and the spectra shown, in order of decreasing absorbance at 650 nm, were taken 33 s (− −), 84 s (—), 193 s (− −), and 22 min (—) after mixing. Inset: direct plot of k_{obs} for the inactivation of H10Q, measured spectrally at 25 °C, *versus* $[H_2O_2]$.

transfer interaction found in the H10Q EH_2 species. In contrast, the $FADH_2$·NAD^+ complex of the C42S peroxidase is essentially isosbestic with the dithionite-reduced enzyme at 450 nm but gives a strong $FADH_2 \rightarrow NAD^+$ charge-transfer band at 740 nm (Parsonage & Claiborne, 1995). On the basis of this comparison with both wild-type and C42S mutant peroxidases, we conclude that the EH_2·NADH spectra shown for the H10Q peroxidase in Figure 3 do not reflect significant contributions from the corresponding EH_4·NAD^+ species.

The redox potential for the wild-type peroxidase EH_2/EH_4 couple has recently been measured at −312 mV at pH 7.0, 23 °C, by titrating the enzyme with NADPH in the presence of 1 mM $NADP^+$ (Crane et al., 1995). Given the E'^0 value of −320 mV for NADH (Loach, 1976), we have concluded that the FAD/$FADH_2$ and NAD^+/NADH potentials are perturbed significantly within the EH_2·NADH complex, leading to a much wider separation and thus stabilizing this redox form. In a similar fashion, the titration data of Figures 3 and 4 suggest that the FAD/$FADH_2$ potential of the H10Q EH_2·NADH complex is significantly lower than that of bound NAD^+/NADH. However, when the free H10Q peroxidase is titrated with NADPH in the presence of $NADP^+$, the potential measured for the EH_2/EH_4 couple is −278 mV; the plot of log $[EH_2]/[EH_4]$ *versus* log $[NADP^+]/[NADPH]$ has a slope of 0.91. It is important to emphasize that, as with wild-type enzyme, at no point in the titration is there any evidence for formation of NADPH or $NADP^+$ complexes with either EH_2 or EH_4 forms of the H10Q mutant. During the first phase of the NADPH titration, the Cys42-SOH redox center is reduced stoichiometrically with each addition of reductant, precluding direct determination of the E/EH_2 potential. We have estimated a value for $E_2 \geq -226$ mV for wild-type enzyme (Crane et al., 1995), and the H10Q titration data suggest that $E_2 \geq -218$ mV, in reasonable agreement. The EH_2/EH_4 potential (E_1) for the H10Q peroxidase is 34 mV more positive than that for wild-type enzyme. Nonetheless, in the corresponding EH_2·NADH complex, the EH_2/EH_4 and NAD^+/NADH potentials are perturbed such that FAD reduction does not occur to a significant extent. This redox behavior parallels that seen with the wild-type peroxidase.

Peroxide Inactivation of H10Q Peroxidase. We have shown that the oxidized wild-type peroxidase is inactivated by H_2O_2; the second-order rate constant for the irreversible process is 8.1 M^{-1} min^{-1} and yields an E(Cys42-SO_3H) form capable of binding NADH but lacking a functional Cys42-SOH redox center (Poole & Claiborne, 1989a; Stehle et al., 1993). We have now repeated this measurement with the recombinant wild-type enzyme, yielding a similar rate constant of 6.5 M^{-1} min^{-1} at pH 7.0, 25 °C. Figure 5 gives the spectral course for the reaction of 2 mM H_2O_2 with the H10Q peroxidase; most noticeable is the loss of the 650 nm absorbance band which we have attributed to the Cys42-SOH→FAD charge-transfer interaction. A similar loss of the low-extinction, long-wavelength absorbance band of the wild-type enzyme was observed during H_2O_2 inactivation as well (Poole & Claiborne, 1989a). Figure 5 also gives the direct plot of k_{obs} values determined spectrally with H10Q at several H_2O_2 concentrations; the second-order rate constant is 314 M^{-1} min^{-1}, representing a 48-fold increase relative to that observed with the wild-type peroxidase. Thus, replacement of His10 by Gln lowers the free energy of activation for the H_2O_2 oxidation of Cys42-SOH by 2.3 kcal/mol.

Steady-State Kinetics of H10Q and H10A Peroxidases. While standard NADH peroxidase assays using a recording spectrophotometer indicated that both His10 mutants were 5−10% as active as wild-type enzyme, we found it difficult to maintain linear initial rates at 340 nm—the enhanced sensitivity toward inactivation by H_2O_2 at millimolar concentrations, as demonstrated with H10Q, is a contributing factor. In addition, we observed that diluted samples of H10Q kept at 4 °C slowly lost up to 30% of their initial activity over ∼3 h. In order to circumvent these problems, initial velocities were measured at 5 °C and at enzyme concentrations of 50−100 nM, using the Applied Photophysics DX.17MV stopped-flow spectrophotometer in both absorbance and fluorescence (at low [NADH]) modes (Crane et al., 1995). At pH 7.0 and 5 °C, the steady-state analysis for H10Q is consistent with the limiting type of ternary complex mechanism recently described for wild-type peroxidase under identical conditions (Crane et al., 1995). The kinetic parameters are compared in Table 1 and reveal that, while k_{cat} is virtually unchanged in the His10 mutants, the

Table 1: Steady-State Kinetic Parameters for NADH Peroxidase H10Q and H10A Mutants and for Wild-Type Enzyme at pH 7.0, 5 °C[a]

	k_{cat} (s^{-1})	K_m(NADH) (μM)	$K_m(H_2O_2)$	V_H/V_D
wild-type	23.3	3.0	14.1 μM	2.4
H10Q	23.7	6.8	0.69 mM	4.3
H10A	27.7	≤12.6	1.0 mM	2.3

[a] Initial velocity measurements were made in 50 mM potassium phosphate, 0.1 M potassium acetate, pH 7.0, plus 0.5 mM EDTA.

$K_m(H_2O_2)$ values are 50- and 70-fold higher, respectively, for H10Q and H10A. The primary deuterium kinetic isotope effect of 4.3 measured with H10Q demonstrates that hydride transfer from NADH remains at least partially rate-limiting in turnover. The pH profile for k_{cat} with wild-type peroxidase indicates a relatively acidic optimum of 5.0−5.5 with an apparent limiting pK_a of 6.9; we have suggested that ionization of Cys42-SOH may contribute to this behavior (Crane et al., 1995). The pH profile for k_{cat} with H10Q is very similar and corresponds to an apparent limiting pK_a of 6.8. Despite the different temperatures at which the wild-type and H10Q k_{cat} profiles were determined (25 and 5 °C, respectively), we can conclude that the apparent pK_a of 6.9 with wild-type peroxidase is not due to His10—His10 is not an essential acid−base catalyst in the peroxidase redox cycle.

Catalytic H_2O_2 Reactivity of H10Q Peroxidase. The pH profile for $k_{cat}/K_m(H_2O_2)$ with the H10Q peroxidase increases linearly over the pH range 5.5−7 and reaches a maximal value of 3.2×10^4 M^{-1} s^{-1} at pH 8.5, 5 °C. At pH 8.5, 5 °C, $k_{cat}/K_m(H_2O_2) = 3.5 \times 10^6$ M^{-1} s^{-1} with wild-type peroxidase (Crane et al., 1995), suggesting that the reaction rate for the H10Q EH_2 form with H_2O_2 is only 1−2% that of wild-type enzyme. Figure 6 gives the stopped-flow traces at 530 and 660 nm which result when H10Q EH_2 is reacted with H_2O_2 under pseudo-first-order conditions; the absorbance changes reflect oxidation of Cys42-SH to Cys42-SOH. Also given in Figure 6 is the direct plot of the k_{obs} values for oxidation at several H_2O_2 concentrations, yielding a second-order rate constant of 1.94 x 10^4 M^{-1} s^{-1} at pH 7.0, 5 °C. This represents a 155-fold decrease relative to the second-order rate constant for the H_2O_2 reaction of wild-type EH_2, determined under identical conditions (Crane et al., 1995). From the second-order rate constants for the H_2O_2 reactions of the wild-type and H10Q EH_2 forms, we can calculate that the replacement of His10 by Gln increases the free energy of activation for peroxide oxidation of Cys42-S^- by 2.8 kcal/mol.

Enzyme-Monitored Turnover with H10A Peroxidase. As shown in Table 1, the steady-state kinetic parameters k_{cat} and V_H/V_D compare very favorably for the wild-type and H10A peroxidases (k_{cat} = 23.3 and 27.7 s^{-1}, and V_H/V_D = 2.4 and 2.3, respectively). Using a stopped-flow spectrophotometer equipped with a diode-array detector (Gassner & Ballou, 1995), we have also demonstrated the presence of an E·NADH complex in steady-state turnover with wild-type enzyme (Crane et al., 1995); further analyses of the reduction of E→EH_2 confirm the rapid formation of this intermediate and indicate that the conversion of E·NADH→EH_2 is subject to a deuterium isotope effect of 3.0. The similarities in k_{cat} *versus* k_{red} values and in V_H/V_D versus k_H/k_D for the wild-type peroxidase indicate that this hydride transfer step is largely rate-limiting in turnover (Crane et al., 1995). Although $K_m(H_2O_2)$ for the H10A mutant is 70-fold higher

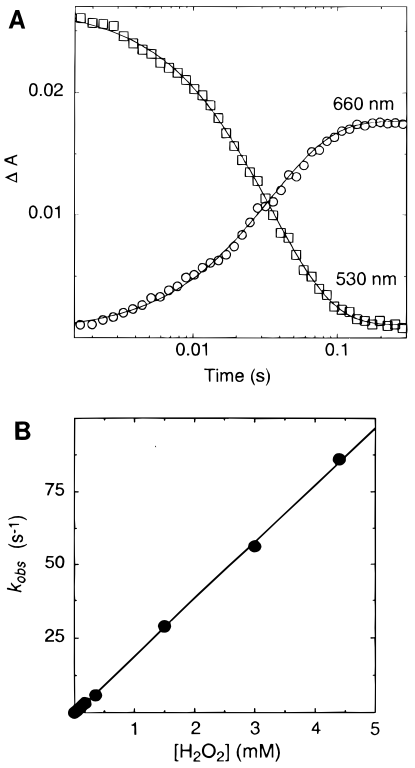

FIGURE 6: Stopped-flow analysis of the reaction of H_2O_2 with H10Q peroxidase EH_2. (A) The H10Q EH_2 form was generated in an aerobic NADH titration and centrifuged 3 times in a CM-30 microconcentrator (Amicon) to remove NAD^+, before introducing into a tonometer. The enzyme (17.5 μM) was then mixed with 1.5 mM H_2O_2 (final concentrations) in the standard pH 7.0 phosphate/acetate buffer at 5 °C, using the Applied Photophysics DX.17MV stopped-flow spectrophotometer. The course of the reaction was monitored at 530 nm (□) and at 660 nm (○). (B) Direct plot of k_{obs} for the oxidation of H10Q EH_2 *versus* [H_2O_2].

than that for the wild-type peroxidase, the very similar values for k_{cat} and V_H/V_D suggest that this hydride transfer step remains largely rate-limiting in H10A. Diode-array analysis of the H10A peroxidase in turnover was performed in the laboratory of Dr. David P. Ballou, University of Michigan, and the result is shown in Figure 7. Although the approach to steady state is slightly more complex than observed with wild-type enzyme, the presence of an oxidized H10A species (evidenced by the λ_{max} at 444 nm) which also displays a distinct long-wavelength maximum at 560 nm in steady-state turnover is quite consistent with the formation of an H10A E·NADH complex. With wild-type peroxidase, the E·NADH species was characterized by an oxidized absorbance maximum at 445 nm with a resolved shoulder at 468 nm and a long-wavelength maximum at 560 nm (Crane et al., 1995); the 560 nm absorbance band is attributed to an NADH→FAD charge-transfer interaction. Since $K_m(H_2O_2)$ for H10A is 1 mM, the enzyme-monitored turnover analysis was repeated at 450 and 660 nm, with 20 mM H_2O_2 (Figure 7), and these data also support the formation of an E·NADH intermediate. The combined spectral and kinetic analyses do, however, indicate that ϵ_{444} for the H10A $E_{steady\text{-}state}$ species is considerably lower than that for the E·NADH intermediate observed when H10A is reduced anaerobically with 1.2 equiv of NADH/FAD. One possible explanation is that the increased $K_m(H_2O_2)$ for the H10A mutant leads to a significant contribution by either EH_2·NADH* and/or EH_2·NADH forms in the $E_{steady\text{-}state}$ spectrum.

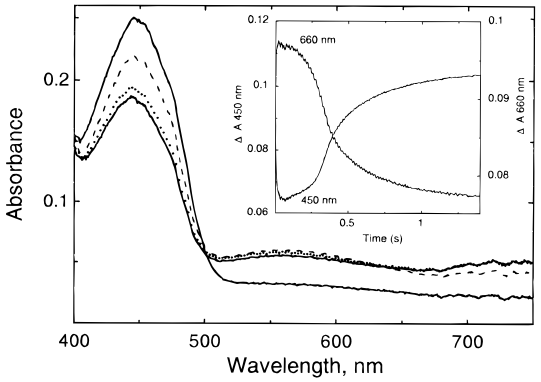

FIGURE 7: Absorption spectra of H10A peroxidase during turnover. The enzyme (23.7 μM) was mixed, under anaerobic conditions, with 0.29 mM NADH and 2 mM H_2O_2 in the standard pH 7.0 phosphate/acetate buffer at 4 °C, using the Hi-Tech SF-61 stopped-flow spectrophotometer equipped with a diode-array detector. Spectra shown, in order of decreasing absorbance at 445 nm, represent E (—) and enzyme at 13.7 ms (— —), 38.7 ms (•••), and 76.2 ms (—) after mixing. Inset: time course for the reaction of H10A peroxidase with NADH and H_2O_2. 15.5 μM E was mixed with 0.11 mM NADH and 20 mM H_2O_2 at pH 7.0, 5 °C, in the Applied Photophysics stopped-flow under anaerobic conditions. The course of the reaction was monitored at 450 nm and at 660 nm.

The value for k_{red} with H10A and NADH at pH 7.0, 5 °C, is 26.7 s^{-1}, and this first-order rate constant is subject to a primary deuterium kinetic isotope effect of 2.2. These values compare very well with the steady-state k_{cat} and V_H/V_D parameters for H10A (27.7 s^{-1} and 2.3, respectively). As previously demonstrated with wild-type NADH peroxidase, the hydride transfer step within the E·NADH complex, yielding EH_2, is also largely rate-limiting with the H10A peroxidase; His10 does not play any essential role in the reduction of E(FAD, Cys42-SOH) to EH_2(FAD, Cys42-SH).

DISCUSSION

Stehle et al. (1993) have proposed that His10 functions as an acid−base catalyst in the enterococcal NADH peroxidase (Scheme 1). Beginning with the E·NADH intermediate described recently by Crane et al. (1995), the neutral His10 imidazole is hydrogen-bonded through NE2 to Cys42-SOH. Reduction to EH_2 by bound NADH yields Cys42-S^-, and His10 is suggested to accept a proton from solvent, forming an ion pair with Cys42-S^-. Rapid binding of NADH gives the EH_2·NADH* complex (Crane et al., 1995), and the reaction with H_2O_2 is proposed to be facilitated by hydrogen-bonding interactions involving Cys42-N, Ser41-N, Ser41-OG, and His10-NE2 and the peroxide oxygens. Nucleophilic attack by Cys42-S^- regenerates Cys42-SOH and the E·NADH complex, as His10 donates its proton to the nascent OH^- to give the product H_2O. This proposed role for His10 has recently been brought into question, however, by Mande et al. (1995), who have observed a hydrogen bond between His10-ND1 and the charged guanidinium group of Arg303 in both the wild-type peroxidase E(Cys42-SO_3H) form (Figure 8) and C42A and C42S mutants. The Arg303-NH2:His10-ND1 distance ranges from 3.0 to 3.2 Å in the three structures, and the positive charge of the guanidinium function is very likely to lower the pK_a of His10, leaving it unprotonated throughout the catalytic cycle.

The present study demonstrates that replacement of His10 with Gln or Ala has little or no effect on k_{cat}, on K_m(NADH), or on the rate of enzyme reduction by NADH. The apparent

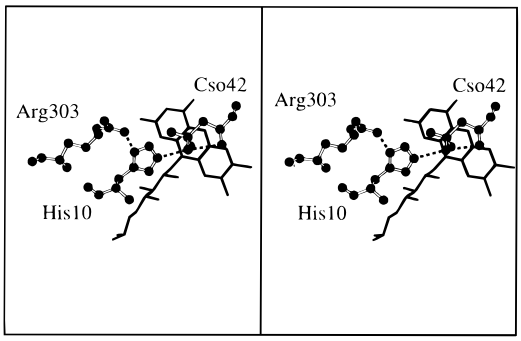

FIGURE 8: Active-site structure of the wild-type peroxidase E(Cys42-SO_3H) form. Shown in stereo is a MOLSCRIPT (Kraulis, 1991) representation including the FAD coenzyme, Cys42-SO_3H, His10, and Arg303. Dashed lines indicate the hydrogen-bonding interactions Cys42-N:Cys42-OX1 (2.8 Å), His10-NE2:Cys42-OX1 (2.8 Å), and Arg303-NH2:His10-ND1 (3.0 Å).

Scheme 1

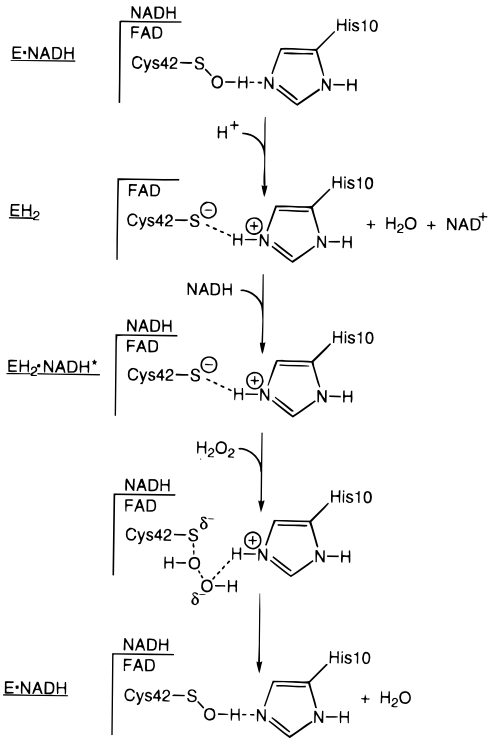

pK_a of 6.9 determined from the pH profile for k_{cat} with wild-type peroxidase is essentially unchanged in the H10Q mutant (apparent pK_a = 6.8); it is clear that protonation of His10 is not responsible for the pH dependence of wild-type enzyme. In contrast, $K_m(H_2O_2)$ is increased 50-fold with H10Q, and the second-order rate constant for the reaction of H_2O_2 with the H10Q EH_2 species (Cys42-S^-) is reduced to 0.6% of the value for wild-type enzyme. We have shown that the steady-state kinetic mechanism is unchanged from that of the wild-type enzyme (Crane et al., 1995), and the initial rate equation is

$$\frac{e}{v_0} = \Phi_0 + \frac{\Phi_1}{[\mathrm{NADH}]} + \frac{\Phi_2}{[\mathrm{H_2O_2}]},$$

$$\text{where } \Phi_0 = \frac{1}{k_{cat}} \text{ and } \frac{\Phi_2}{\Phi_0} = K_m(\mathrm{H_2O_2})$$

Since the k_{cat} values for wild-type and H10Q peroxidases are very similar, the 50-fold increase in $K_m(H_2O_2)$ must reflect an increase in the mutant Φ_2 parameter. We have

Scheme 2

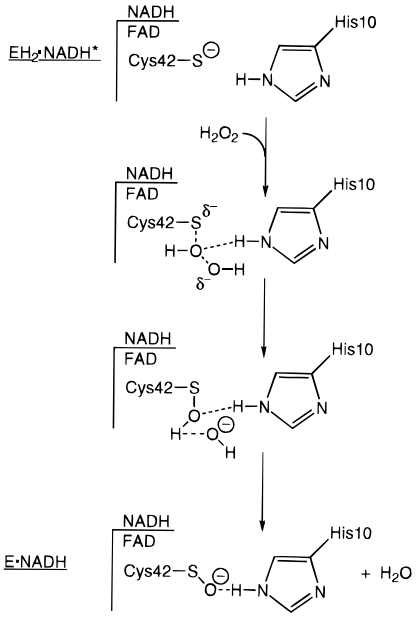

previously shown that $\Phi_2 = 1/k_3$, where k_3 is the second-order rate constant for the reaction of EH_2·NADH* with H_2O_2 (measured as the reaction $EH_2 + H_2O_2 \rightarrow E + H_2O$; Crane et al., 1995). The experimentally-determined value of $k_3 = 1.94 \times 10^4$ M^{-1} s^{-1} for the H10Q peroxidase compares very favorably with that calculated ($k_3 = 3.4 \times 10^4$ M^{-1} s^{-1}) from the steady-state parameters.

Replacement of His10 by Gln therefore results in a 2.8 kcal/mol increase in the free energy of activation for the reaction between EH_2 Cys42-S^- and H_2O_2. While crystallographic evidence and kinetic evidence are not consistent with an essential role for this residue as an acid−base catalyst, the extent of transition state stabilization associated with His10 in the H_2O_2 reaction is suggestive of a favorable hydrogen-bonding interaction between the neutral imidazole (mediated by NE2-H) and the peroxide oxygen(s) (Scheme 2). Fersht et al. (1985) have shown that an unfavorable free energy change of 0.5−1.5 kcal/mol is observed on deletion of a hydrogen bond between uncharged groups on enzyme and substrate; if a charged group on the substrate is involved, deletion of the hydrogen bond may weaken the interaction by ∼3.5−4.5 kcal/mol. In addition to the hydrogen bond observed between His10-NE2 and the OX1 oxygen of Cys42-SO_3H in the wild-type NADH peroxidase structure (Stehle et al., 1993), Mande et al. (1995) have shown that His10-NE2 is hydrogen-bonded to an active-site water molecule (WAT453) in the C42S mutant. This solvent molecule has a low *B* factor of 12.6 Å^2 and is displaced by OX1 in the wild-type structure; it is possible that WAT453, which is also hydrogen-bonded to Ser42-OG in the mutant, approximates the position of the proximal peroxide oxygen during the nucleophilic attack of Cys42-S^- on H_2O_2. The hydrogen-bonding network for this tightly-bound water also includes Ser41-N, Ser42-N (in the C42S mutant; Cys42-N forms a hydrogen bond with OX1 in the wild-type structure), and FAD-O2′F and could be involved in stabilization of the developing negative charge on the oxygens of the H_2O_2 substrate. The very similar results obtained with both H10Q and H10A peroxidases indicate that Gln is not an effective hydrogen-bonding replacement for His10 in this context.

We have suggested (Claiborne et al., 1993) that His10, through its hydrogen-bonding interaction with Cys42-SOH (seen in the crystal structure as Cys42-SO_3H), also serves to stabilize this unusual redox center. The 50-fold increase in the second-order rate constant for H_2O_2 inactivation of the H10Q peroxidase, which involves the irreversible oxidation of Cys42-SOH→Cys42-sulfinic (-SO_2H) and/or sulfonic (-SO_3H) acid derivatives (Poole & Claiborne, 1989a), provides further support for this conclusion. In this case, replacement of His10 with Gln lowers the free energy of activation by 2.3 kcal/mol; we would suggest that this change represents a destabilization of the ground state Cys42-SOH due to the absence of the His10-NE2 hydrogen bond. In addition, the strong enhancement of the 650 nm charge-transfer band for the Cys42-SOH form of the H10Q peroxidase supports earlier conclusions regarding the intrinsic long-wavelength absorbance of the oxidized wild-type enzyme (Poole & Claiborne, 1989a). The electron-rich oxygens of bound phenolic ligands, in their anionic phenolate forms, serve as charge-transfer donors to the FMN in Old Yellow Enzyme, for example (Abramovitz & Massey, 1976). The 2.0 Å structure of the Old Yellow Enzyme complex with *p*-hydroxybenzaldehyde reveals the presence of two hydrogen bonds to the phenolate oxygen involving unprotonated His191-NE2 and Asn194-ND2 (Fox & Karplus, 1994). A similar stabilization of the anionic Cys42-SO^- in the wild-type NADH peroxidase is likely to be promoted by interaction with His10; replacement of His with Gln or Ala has pronounced effects on the spectral properties of the Cys42-SO^-→FAD charge-transfer interaction.

It is also clear from this work that His10 replacement does not have a detectable effect on the pK_a of Cys42-SH in the EH_2 form of the peroxidase. Furthermore, our earlier suggestion, that the apparent pK_a of 6.9 measured with the wild-type peroxidase from the pH dependence of k_{cat} could be attributed to Cys42-SOH (Crane et al., 1995), should be re-evaluated in view of the pH-independent nature of the oxidized H10Q charge-transfer band over the range 5.4−7.1. Additional structural studies are currently being carried out in collaboration with Dr. Wim Hol of the University of Washington to address the questions raised by these observations.

ACKNOWLEDGMENT

We thank Dr. David P. Ballou, Department of Biological Chemistry, University of Michigan, for providing access to the diode-array stopped-flow spectrophotometer in his laboratory and for his guidance and helpful discussions during the course of those experiments. We also thank Dr. Joanne Yeh, Department of Biological Structure, University of Washington, for kindly providing Figure 8.

REFERENCES

Abramovitz, A. S., & Massey, V. (1976) *J. Biol. Chem. 251*, 5327−5336.

Bull, C., & Ballou, D. P. (1981) *J. Biol. Chem. 256*, 12673−12680.

Claiborne, A., Miller, H., Parsonage, D., & Ross, R. P. (1993) *FASEB J. 7*, 1483−1490.

Claiborne, A., Ross, R. P., Ward, D., Parsonage, D., & Crane, E. J., III (1994) in *Flavins and Flavoproteins 1993* (Yagi, K., Ed.) pp 587−596, de Gruyter, New York.

Crane, E. J., III, Parsonage, D., Poole, L. B., & Claiborne, A. (1995) *Biochemistry 34*, 14114−14124.

Dawson, R. M. C., Elliott, D. C., Elliott, W. H., & Jones, K. M. (1986) *Data for Biochemical Research*, 3rd ed., pp 16−17, Clarendon Press, Oxford.
Fersht, A. R., Shi, J.-P., Knill-Jones, J., Lowe, D. M., Wilkinson, A. J., Blow, D. M., Brick, P., Carter, P., Waye, M. M. Y., & Winter, G. (1985) *Nature 314*, 235−238.
Fox, K. M., & Karplus, P. A. (1994) *Structure 2*, 1089−1105.
Fraser, C. M., Gocayne, J. D., White, O., Adams, M. D., Clayton, R. A., Fleischmann, R. D., Bult, C. J., Kerlavage, A. R., Sutton, G., Kelley, J. M., Fritchman, J. L., Weidman, J. F., Small, K. V., Sandusky, M., Fuhrmann, J., Nguyen, D., Utterback, T. R., Saudek, D. M., Phillips, C. A., Merrick, J. M., Tomb, J.-F., Dougherty, B. A., Bott, K. F., Hu, P.-C., Lucier, T. S., Peterson, S. N., Smith, H. O., Hutchison, C. A., III, & Venter, J. C. (1995) *Science 270*, 397−403.
Gassner, G. T., & Ballou, D. P. (1995) *Biochemistry 34*, 13460−13471.
Greer, S., & Perham, R. N. (1986) *Biochemistry 25*, 2736−2742.
Kraulis, P. J. (1991) *J. Appl. Crystallogr. 24*, 946−950.
Loach, P. A. (1976) in *Handbook of Biochemistry and Molecular Biology* (Fasman, G. D., Ed.) 3rd ed., Vol. I, pp 122−130, CRC Press, Boca Raton, FL.
Mande, S. S., Parsonage, D., Claiborne, A., & Hol, W. G. J. (1995) *Biochemistry 34*, 6985−6992.
March, J. (1985) *Advanced Organic Chemistry*, 3rd ed., p 221, John Wiley & Sons, New York.
Matsumoto, J., Higuchi, M., Shimada, M., Yamamoto, Y., & Kamio, Y. (1995) *Biosci., Biotechnol., Biochem. 60* (in press).
Miller, H., Poole, L. B., & Claiborne, A. (1990) *J. Biol. Chem. 265*, 9857−9863.
Miller, H., Mande, S. S., Parsonage, D., Sarfaty, S. H., Hol, W. G. J., & Claiborne, A. (1995) *Biochemistry 34*, 5180−5190.
Mittl, P. R. E., & Schulz, G. E. (1994) *Protein Sci. 3*, 799−809.
Parsonage, D., & Claiborne, A. (1995) *Biochemistry 34*, 435−441.
Parsonage, D., Miller, H., Ross, R. P., & Claiborne, A. (1993) *J. Biol. Chem. 268*, 3161−3167.
Poole, L. B., & Claiborne, A. (1986) *J. Biol. Chem. 261*, 14525−14533.
Poole, L. B., & Claiborne, A. (1989a) *J. Biol. Chem. 264*, 12330−12338.
Poole, L. B., & Claiborne, A. (1989b) *J. Biol. Chem. 264*, 12322−12329.
Rietveld, P., Arscott, L. D., Berry, A., Scrutton, N. S., Deonarain, M. P., Perham, R. N., & Williams, C. H., Jr. (1994) *Biochemistry 33*, 13888−13895.
Ross, R. P., & Claiborne, A. (1991) *J. Mol. Biol. 221*, 857−871.
Ross, R. P., & Claiborne, A. (1992) *J. Mol. Biol. 227*, 658−671.
Stehle, T., Ahmed, S. A., Claiborne, A., & Schulz, G. E. (1991) *J. Mol. Biol. 221*, 1325−1344.
Stehle, T., Claiborne, A., & Schulz, G. E. (1993) *Eur. J. Biochem. 211*, 221−226.
Tripolt, R., Belaj, F., & Nachbaur, E. (1993) *Z. Naturforsch. 48B*, 1212−1222.
Williams, C. H., Jr. (1992) in *Chemistry and Biochemistry of Flavoenzymes* (Müller, F., Ed.) Vol. III, pp 121−211, CRC Press, Boca Raton, FL.

BI952347Y